

Time-dependent optimized coupled-cluster method for multielectron dynamics II. A coupled electron-pair approximation

Himadri Pathak,^{1, a)} Takeshi Sato,^{1, 2, 3, b)} and Kenichi L. Ishikawa^{1, 2, 3, c)}

¹⁾Department of Nuclear Engineering and Management, School of Engineering, The University of Tokyo, 7-3-1 Hongo, Bunkyo-ku, Tokyo 113-8656, Japan

²⁾Photon Science Center, School of Engineering, The University of Tokyo, 7-3-1 Hongo, Bunkyo-ku, Tokyo 113-8656, Japan

³⁾Research Institute for Photon Science and Laser Technology, The University of Tokyo, 7-3-1 Hongo, Bunkyo-ku, Tokyo 113-0033, Japan

(Dated: 8 January 2020)

We report the implementation of a cost-effective approximation method within the framework of time-dependent optimized coupled-cluster (TD-OCC) method [J. Chem. Phys. **148**, 051101 (2018)] for real-time simulations of intense laser-driven multielectron dynamics. The method, designated as TD-OCEPA0, is a time-dependent extension of the simplest version of the coupled-electron pair approximation with optimized orbitals [J. Chem. Phys. **139**, 054104 (2013)]. It is size extensive, gauge invariant, and computationally much more efficient than the TD-OCC with double excitations (TD-OCCD). We employed this method to simulate the electron dynamics in Ne and Ar atoms exposed to intense near infrared laser pulses with various intensities. The computed results, including high-harmonic generation spectra and ionization yields, are compared with those of various other methods ranging from uncorrelated time-dependent Hartree-Fock (TDHF) to fully-correlated (within the active orbital space) time-dependent complete-active-space self-consistent-field (TD-CASSCF). The TD-OCEPA0 results show a good agreement with TD-CASSCF ones for moderate laser intensities. For higher intensities, however, TD-OCEPA0 tends to overestimate the correlation effect, as occasionally observed for CEPA0 in the ground-state correlation energy calculations.

I. INTRODUCTION

In recent years there has been a significant breakthrough in the experimental techniques to measure and control the motions of electrons in atoms and molecules, for example, measurement of the delay in photoionization^{1,2}, migration of charge in a chemical process^{3,4} and dynamical change of the orbital picture during the course of bond breaking or formation⁵⁻⁷. Atoms and molecules interacting with laser pulses of intensity 10^{14} W/cm² or higher in the visible to mid-infrared region, show highly nonlinear response to the fields such as above-threshold ionization (ATI), tunneling ionization, nonsequential double ionization (NSDI) and high-harmonic generation (HHG). All these phenomena are by nature nonperturbative⁸. The essence of the attosecond science lies in the HHG⁹⁻¹¹, one of the most successful means to generate ultrashort coherent light pulses in the wavelength ranging from extreme-ultraviolet (XUV) to the soft x-ray regions¹²⁻¹⁵, which can be used to unravel the electronic structure^{5,6} or dynamics^{4,16} of many-body quantum systems. The HHG spectrum is characterized by a plateau where the intensity of the emitted light remains nearly constant up to many orders, followed by a sharp cutoff¹⁷.

A whole lot of numerical methods have been developed to understand atomic and molecular dynamics in the intense laser field (For a comprehensive review on various wavefunction-based methods for the study of laser-induced electron dynamics, see Ref. 18) to catch up with the progress

in the experimental techniques. In principle, “the best” one could do is to solve the time-dependent Schrödinger equation (TDSE) to have an exact description. However, the exact solution of the TDSE is not feasible for systems containing more than two electrons¹⁹⁻²⁸. As a consequence, single-active electron (SAE) approximation has been widely used, in which the outermost electron is explicitly treated with the effect of the other electrons modeled by an effective potential. The SAE model has been successful in numerically exploring various high-field phenomena^{29,30}. However, the missing electron correlation in SAE makes this method at best qualitative.⁷

Among other established methods, the multiconfiguration time-dependent Hartree-Fock (MCTDHF)³¹⁻³⁵ and time-dependent complete-active-space self-consistent-field (TD-CASSCF)³⁶⁻³⁸ are the most competent theoretical methods for the study of the laser-driven multielectron dynamics where both configuration interaction (CI) coefficients and the orbitals are propagated in time. The time-dependent (or *optimized* in the sense of time-dependent variational principle) orbital formulation widens the applicability of these methods by allowing to use a fewer number of orbitals than the case of fixed orbital treatments. Though powerful, the dilemma with these full CI-based methods is the applicability to large atomic or molecular systems due to the factorial escalation of the computational cost with respect to the number of electrons. To subjugate this difficulty, more approximate, thus computationally more efficient time-dependent multiconfiguration self-consistent-field (TD-MCSCF) methods have been developed, based on the truncated CI expansion within the chosen active orbital space³⁹⁻⁴², compromising size extensivity.

To regain the size extensivity, the coupled-cluster expansion⁴³⁻⁴⁵ of the time-dependent wavefunction emerges

^{a)}Electronic mail: pathak@atto.t.u-tokyo.ac.jp

^{b)}Electronic mail: sato@atto.t.u-tokyo.ac.jp

^{c)}Electronic mail: ishiken@n.t.u-tokyo.ac.jp

naturally as an alternative to the truncated CI expansion. The initial ideas of developing time-dependent coupled-cluster go back to as early as 1978 by Schönhammer and Gunnarsson⁴⁶, and Hoodbhoy and Negele^{47,48}. Here we take note of a few theoretical works on the time-dependent coupled-cluster method for time-independent Hamiltonian^{49–53} and a few recent applications of the method with fixed orbitals^{54,55}. Huber and Klamroth⁵⁶ were the first to apply the coupled-cluster method (with single and double excitations) to laser-driven dynamics of molecules, using time-independent orbitals and the CI wavefunction reconstructed from the propagated CC amplitudes to evaluate the expectation value of operators.

In 2012, Kvaal pioneered a time-dependent coupled-cluster method using time-dependent orbitals for electron dynamics, designated as orbital-adaptive time-dependent coupled-cluster (OATDCC) method⁵⁷. Based on Arponen’s bi-orthogonal formulation of the coupled-cluster theory⁵⁸, the OATDCC method is derived from the complex-analytic action functional using time-dependent biorthonormal orbitals. Recently, we have also developed time-dependent optimized coupled-cluster (TD-OCC) method⁵⁹ based on the real action functional using time-dependent orthonormal orbitals. The TD-OCC method is a time-dependent extension of the orbital optimized coupled-cluster method popular in the stationary electronic structure theory^{60–63}. It is not only size extensive, but also gauge invariant, and scales polynomially with respect to the number of active electrons N . Theoretical as well as numerical comparison of closely-related OATDCC and TD-OCC methods is yet to be done, and will be discussed elsewhere. (See Refs. 64 and 65 for recent theoretical accounts on orbital-optimized and time-dependent coupled-cluster methods, and Refs. 66 and 67 for the gauge-invariant coupled-cluster response theory with orthonormal and biorthonormal orbitals, respectively.)

We have implemented TD-OCC method with double excitations (TD-OCCD) and double and triple excitations (TD-OCCDT) within the chosen active space⁵⁹, of which the computational cost scales as N^6 and N^8 , respectively. Such scalings are milder than the factorial one in the MCTDHF and TD-CASSCF methods; nevertheless, a lower cost alternative within the TD-OCC framework is highly appreciated to further extend the applicability to heavier atoms and larger molecules interacting with intense laser fields.

One such low-cost model is a family of the methods called coupled-electron pair approximation (CEPA), originally introduced in 1970’s^{68–74}. In particular, the simplest version of the family, denoted as CEPA0 (See Sec. II for the definition.), is recently attracting a renewed attention^{75–78} due to its high cost-performance balance. The orbital-optimized version of this method (OCEPA0) has been also developed and applied to the calculation of, e.g. equilibrium geometries and harmonic vibrational frequencies of molecules⁷⁹, which motivated us to extend it to the time-dependent problem.

In the present article, we report the implementation of the time-dependent, orbital-optimized version of the CEPA0 theory, hereafter referred to as TD-OCEPA0. Pilot applications to the simulation of induced dipole moment, high-harmonic spectra, and ionization probability in three different laser

intensities for Ne and Ar are reported. We compare TD-OCEPA0 results with those of other methods ranging from uncorrelated TDHF, TD-MCSCF with a truncated CI expansion, TD-OCCD, and fully correlated TD-CASSCF, using the same number of active orbitals (except for TDHF) to quantitatively explore the performance of TD-OCEPA0. The computational cost of TD-OCEPA0 scales as N^6 , which is formally the same as that of TD-OCCD; however as shown in Sec. II, one need not solve for the double deexcitation operator Λ_2 , but it is sufficient to propagate the double excitation operator T_2 since $\Lambda_2 = T_2^\dagger$. This leads to a great saving of the computational time as numerically demonstrated in Sec. III.

The manuscript is arranged as follows. A concise description of the TD-OCEPA0 method is presented in Sec. II. Section III discusses the computational results. Finally, we made our concluding remark in Sec. IV. We use Hartree atomic units unless stated otherwise, and Einstein convention is implied throughout for summation over orbital indices.

II. METHOD

A. Background

We consider a system with N electrons governed by the following Hamiltonian,

$$H = \sum_{i=1}^N h(\mathbf{r}_i, \mathbf{p}_i) + \sum_{i=1}^{N-1} \sum_{j=2}^N \frac{1}{|\mathbf{r}_i - \mathbf{r}_j|}, \quad (1)$$

where \mathbf{r}_i and \mathbf{p}_i are the position and canonical momentum of an electron i . The corresponding second quantized Hamiltonian reads

$$\hat{H} = h_\nu^\mu \hat{E}_\nu^\mu + \frac{1}{2} u_{\nu\lambda}^{\mu\gamma} \hat{E}_{\nu\lambda}^{\mu\gamma}, \quad (2)$$

where $\hat{E}_\nu^\mu = \hat{c}_\mu^\dagger \hat{c}_\nu$ and $\hat{E}_{\nu\lambda}^{\mu\gamma} = \hat{c}_\mu^\dagger \hat{c}_\lambda^\dagger \hat{c}_\gamma \hat{c}_\nu$, with \hat{c}_μ^\dagger (\hat{c}_μ) being a creation (annihilation) operator in a complete, orthonormal set of $2n_{\text{bas}}$ spin-orbitals $\{\psi_\mu\}$, where n_{bas} is the number of basis functions (or the number of grid points) to expand the spatial part of ψ_μ , and

$$h_\nu^\mu = \int dx_1 \psi_\mu^*(x_1) h(\mathbf{r}_1, \mathbf{p}_1) \psi_\nu(x_1), \quad (3)$$

$$u_{\nu\lambda}^{\mu\gamma} = \int \int dx_1 dx_2 \frac{\psi_\mu^*(x_1) \psi_\gamma^*(x_2) \psi_\nu(x_1) \psi_\lambda(x_2)}{|\mathbf{r}_1 - \mathbf{r}_2|}, \quad (4)$$

where $x_i = (\mathbf{r}_i, \sigma_i)$ is a composite spatial-spin coordinate.

The complete set of $2n_{\text{bas}}$ spin-orbitals (labeled with $\mu, \nu, \gamma, \lambda$) is divided into n_{occ} *occupied* (o, p, q, r, s) and $2n_{\text{bas}} - n_{\text{occ}}$ *virtual* spin-orbitals having nonzero and vanishing occupations, respectively, in the coupled-cluster (or MCSCF) expansion of the total wavefunction. The occupied spin-orbitals are classified into n_{core} *core* spin-orbitals which are occupied in the reference Φ and kept uncorrelated, and $n_{\text{act}} = n_{\text{occ}} - n_{\text{core}}$ *active* spin-orbitals (t, u, v, w) among which the $N_{\text{act}} = N - n_{\text{core}}$ active electrons are correlated.

The active spin-orbitals are further splitted into those in the *hole* space (i, j, k, l) and the *particle* space (a, b, c, d), which are occupied and unoccupied, respectively, in Φ . The core spin-orbitals can also be splitted into those in the *frozen-core* space (i'', j'') which are fixed in time, and the *dynamical-core* space (i', j') which are propagated in time³⁶.

Hereafter we refer to spin-orbitals simply as orbitals. [Note that Refs. 36,37,42 for TD-MCSCF methods deal with the equations of motion (EOMs) for spatial orbitals.] The system Hamiltonian (2) is equivalently written as

$$\hat{H} = E_0 + f_\nu^\mu \{\hat{E}_\nu^\mu\} + \frac{1}{4} v_{\nu\lambda}^{\mu\gamma} \{\hat{E}_{\nu\lambda}^{\mu\gamma}\}, \quad (5)$$

where $E_0 = \langle \Phi | \hat{H} | \Phi \rangle$, $f_\nu^\mu = h_\nu^\mu + v_{\nu j}^{\mu j}$ (j running over core and hole spaces), $v_{\nu\lambda}^{\mu\gamma} = v_{\nu\lambda}^{\mu\gamma} - v_{\lambda\nu}^{\mu\gamma}$, and the bracket $\{\dots\}$ implies that the operator inside is normal ordered relative to the reference.

B. Review of TD-OCC method

Let us begin with a generic TD-OCC framework, which relies on the time-dependent variational principle with real action functional⁵⁹,

$$S = \text{Re} \int_{t_0}^{t_1} L dt = \frac{1}{2} \int_{t_0}^{t_1} (L + L^*) dt, \quad (6)$$

$$L = \langle \Phi | (1 + \hat{\Lambda}) e^{-\hat{T}} (\hat{H} - i \frac{\partial}{\partial t}) e^{\hat{T}} | \Phi \rangle, \quad (7)$$

where

$$\hat{T} = \hat{T}_2 + \hat{T}_3 \dots = \tau_{ij}^{ab} \hat{E}_{ij}^{ab} + \tau_{ijk}^{abc} \hat{E}_{ijk}^{abc} \dots, \quad (8)$$

$$\hat{\Lambda} = \hat{\Lambda}_2 + \hat{\Lambda}_3 \dots = \lambda_{ab}^{ij} \hat{E}_{ab}^{ij} + \lambda_{abc}^{ijk} \hat{E}_{abc}^{ijk} \dots, \quad (9)$$

with $\tau_{ij\dots}^{ab\dots}$ and $\lambda_{ab\dots}^{ij\dots}$ being excitation and deexcitation amplitudes, respectively. We require that the action to be stationary, $\delta S = 0$, with respect to the variation of amplitudes $\delta \tau_{ij\dots}^{ab\dots}$, $\delta \lambda_{ab\dots}^{ij\dots}$ and orthonormality-conserving orbital variations $\delta \psi_\mu = \psi_\nu \Delta_\mu^\nu$, with antiHermitian matrix elements $\Delta_\mu^\nu \equiv \langle \psi_\nu | \delta \psi_\mu \rangle$.

To facilitate formulation of TD-OCEPA0 below, we transform the Lagrangian into two equivalent expressions,

$$L = L_0 + \langle \Phi | (1 + \hat{\Lambda}) [\{\hat{H} - i\hat{X}\} e^{\hat{T}}]_c | \Phi \rangle - i \lambda_{ab\dots}^{ij\dots} \dot{\tau}_{ij\dots}^{ab\dots}, \quad (10a)$$

$$= (h_q^p - i X_q^p) \rho_p^q + \frac{1}{2} v_{qs}^{pr} \rho_{pr}^{qs} - i \lambda_{ab\dots}^{ij\dots} \dot{\tau}_{ij\dots}^{ab\dots}, \quad (10b)$$

where $\hat{X} = X_\nu^\mu \hat{E}_\nu^\mu$ with $X_\nu^\mu = \langle \psi_\mu | \dot{\psi}_\nu \rangle$ being antiHermitian, $L_0 = \langle \Phi | (\hat{H} - i\hat{X}) | \Phi \rangle$, and the symbol $[\dots]_c$ indicates the restriction to diagrammatically connected terms. The one-electron and two-electron reduced density matrices (RDMs) ρ_p^q and ρ_{pr}^{qs} are defined, respectively, by

$$\rho_p^q = \langle \Phi | (1 + \hat{\Lambda}) e^{-\hat{T}} \hat{E}_q^p e^{\hat{T}} | \Phi \rangle, \quad (11)$$

$$\rho_{pr}^{qs} = \langle \Phi | (1 + \hat{\Lambda}) e^{-\hat{T}} \hat{E}_{qs}^{pr} e^{\hat{T}} | \Phi \rangle. \quad (12)$$

To benefit later discussions, we separate the one-electron and two-electron RDMs (1RDM and 2RDM, respectively) into reference and correlation contributions,

$$\rho_p^q = (\rho_0)_p^q + \gamma_p^q, \quad (13)$$

$$\rho_{pr}^{qs} = (\rho_0)_{pr}^{qs} + \gamma_{pr}^{qs}, \quad (14)$$

where the reference contributions $(\rho_0)_p^q = \delta_j^q \delta_p^j$ and $(\rho_0)_{pr}^{qs} = \gamma_p^q \delta_j^s \delta_r^j + \gamma_r^s \delta_j^q \delta_p^j - \gamma_r^q \delta_j^s \delta_p^j - \gamma_p^s \delta_j^q \delta_r^j + \delta_j^q \delta_p^j \delta_k^s \delta_r^k - \delta_j^s \delta_p^j \delta_k^q \delta_r^k$ (j, k running over core and hole spaces) are independent of the correlation treatment, and the correlation contributions are defined as

$$\gamma_p^q = \langle \Phi | (1 + \hat{\Lambda}) [\{\hat{E}_q^p\} e^{\hat{T}}]_c | \Phi \rangle, \quad (15a)$$

$$\gamma_{pr}^{qs} = \langle \Phi | (1 + \hat{\Lambda}) [\{\hat{E}_{qs}^{pr}\} e^{\hat{T}}]_c | \Phi \rangle. \quad (15b)$$

See Ref. 59 for the derivation of general TD-OCC EOMs based on the real-valued action principle outlined here.

C. TD-OCEPA0 method

Now we define the TD-OCEPA0 method by (i) including double (de)excitations only ($\hat{T} = \hat{T}_2$, $\hat{\Lambda} = \hat{\Lambda}_2$) and (ii) linearizing the exponential operator $e^{\hat{T}_2}$, in the normal-ordered, connected expression of the coupled-cluster Lagrangian [Eq. (10a)],

$$L = L_0 + \langle \Phi | (1 + \hat{\Lambda}_2) [\{\hat{H} - i\hat{X}\} (1 + \hat{T}_2)]_c | \Phi \rangle - i \lambda_{ab}^{ij} \dot{\tau}_{ij}^{ab}, \quad (16)$$

and, accordingly the correlation RDMs [Eqs. (15)],

$$\gamma_p^q = \langle \Phi | (1 + \hat{\Lambda}_2) [\{\hat{E}_q^p\} (1 + \hat{T}_2)]_c | \Phi \rangle, \quad (17a)$$

$$\gamma_{pr}^{qs} = \langle \Phi | (1 + \hat{\Lambda}_2) [\{\hat{E}_{qs}^{pr}\} (1 + \hat{T}_2)]_c | \Phi \rangle. \quad (17b)$$

Requiring $\delta S / \delta \lambda_{ab}^{ij}(t) = 0$ and $\delta S / \delta \tau_{ij}^{ab}(t) = 0$, respectively, using L of Eq. (16) derives

$$\begin{aligned} i \dot{\tau}_{ij}^{ab} &= \langle \Phi | \hat{E}_{ab}^{ij} [\{\hat{H} - i\hat{X}\} (1 + \hat{T}_2)]_c | \Phi \rangle \\ &= v_{ij}^{ab} - p(ij) \bar{f}_j^k \tau_{ik}^{ab} + p(ab) \bar{f}_c^a \tau_{ij}^{cb} \\ &\quad + \frac{1}{2} v_{cd}^{ab} \tau_{ij}^{cd} + \frac{1}{2} v_{ij}^{kl} \tau_{kl}^{ab} + p(ij) p(ab) v_{ic}^{ak} \tau_{kj}^{cb}, \end{aligned} \quad (18)$$

$$\begin{aligned} -i \dot{\lambda}_{ab}^{ij} &= \langle \Phi | (1 + \hat{\Lambda}_2) [\{\hat{H} - i\hat{X}\} \hat{E}_{ij}^{ab}]_c | \Phi \rangle \\ &= v_{ab}^{ij} - p(ij) \bar{f}_i^k \lambda_{ab}^{kj} + p(ab) \bar{f}_a^c \lambda_{cb}^{ij} \\ &\quad + \frac{1}{2} v_{ab}^{cd} \lambda_{cd}^{ij} + \frac{1}{2} v_{kl}^{ij} \lambda_{ab}^{kl} + p(ij) p(ab) v_{kb}^{cj} \lambda_{ac}^{ik}, \end{aligned} \quad (19)$$

where $\bar{f}_q^p = f_q^p - i X_q^p$, and $p(\mu\nu)$ is the anti-symmetrizer; $p(\mu\nu) A_{\mu\nu} = A_{\mu\nu} - A_{\nu\mu}$. Comparing Eqs (18) and (19), and noting that the orbitals are orthonormal, one sees that the EOM for λ_{ab}^{ij} is the complex conjugate of that for τ_{ij}^{ab} , concluding that $\hat{\Lambda}_2 = \hat{T}_2^\dagger$. As a result, the first and second terms of Eq. (16) are real, and

$$\begin{aligned} \text{Im} \int_{t_0}^{t_1} L dt &= \frac{1}{2i} \int_{t_0}^{t_1} (L - L^*) dt \\ &= \frac{1}{2} \left\{ |\tau_{ij}^{ab}(t_1)|^2 - |\tau_{ij}^{ab}(t_0)|^2 \right\} \end{aligned} \quad (20)$$

is independent of the integration path and irrelevant in taking its variation. Therefore, *given the orthonormal orbitals*, L is essentially real, and one could equally base oneself on

$$S = \int_{t_0}^{t_1} L dt, \quad (21)$$

for TD-OCEPA0 ansatz. See Sec. IID below for more explicit account of this point.

Based on the natively real action functional S of Eq. (21), the equation for $X_\nu^\mu = \langle \psi_\mu | \dot{\psi}_\nu \rangle$ is derived by requiring $\delta S / \delta \Delta_\nu^\mu = 0$ using the Lagrangian expression of Eq. (10b) and RDMs of Eqs. (17) to obtain

$$i(X_p^\nu \rho_\mu^\nu - \rho_p^\nu X_\mu^\nu) = F_p^\nu \rho_\mu^\nu - \rho_p^\nu F_p^{\mu*}, \quad (22)$$

where $F_p^\mu = \langle \psi_\mu | \hat{F} | \psi_p \rangle$,

$$\hat{F} | \psi_p \rangle = \hat{h} | \psi_p \rangle + \hat{W}_s^r | \psi_q \rangle \rho_{or}^{qs} (\rho^{-1})_p^o, \quad (23)$$

$$W_s^r(x_1) = \int dx_2 \frac{\psi_r^*(x_2) \psi_s(x_2)}{|\mathbf{r}_1 - \mathbf{r}_2|}. \quad (24)$$

Subsequent analyses of Eq. (22) are parallel to those for TD-MCSCF methods^{39,42}, and one arrives at the orbital EOMs,

$$i|\dot{\psi}_p\rangle = (\hat{1} - \hat{P})\hat{F}|\psi_p\rangle + |\psi_q\rangle X_p^q, \quad (25)$$

where $\hat{1}$ is the identity operator within the orbital space $\{\psi_\mu\}$, and $\hat{P} = \sum_q |\psi_q\rangle\langle\psi_q|$, with non-redundant orbital rotations determined by

$$i(\delta_u^t - \rho_u^t)X_{i'}^u = F_{i'}^t - \rho_u^t F_u^{i'*}, \quad (26)$$

$$i(X_j^a \rho_i^j - \rho_b^a X_i^b) = F_j^a \rho_i^j - \rho_b^a F_b^{j*}. \quad (27)$$

A careful consideration of the frozen-core orbitals within the electric dipole approximation derives

$$iX_\mu^{i''} = \begin{cases} 0 & \text{(length gauge)} \\ \mathbf{E}(t) \cdot \langle \psi_{i''} | \mathbf{r} | \psi_\mu \rangle & \text{(velocity gauge)} \end{cases}, \quad (28)$$

where \mathbf{E} is the external electric field, enabling gauge-invariant simulations with frozen-core orbitals.³⁷

Redundant orbital rotations $\{X_{j'}^i\}$, $\{X_j^i\}$, and, $\{X_b^a\}$ can be arbitrary antiHermitian matrix elements. In particular, if one chooses $X_b^a = X_j^i = 0$, the term $-i\hat{X}$ is dropped in Eqs. (18) and (19). Again as a consequence of $\hat{\Lambda}_2 = \hat{T}_2^\dagger$, both 1RDM and 2RDM are Hermitian, of which the algebraic expression of non-zero elements are given by

$$\gamma_i^j = -\frac{1}{2}\lambda_{cd}^{kj}\tau_{ki}^{cd}, \gamma_a^b = \frac{1}{2}\lambda_{ca}^{kl}\tau_{kl}^{cb}, \quad (29a)$$

$$\gamma_{ab}^{cd} = \frac{1}{2}\lambda_{ab}^{kl}\tau_{kl}^{cd}, \gamma_{ij}^{kl} = \frac{1}{2}\lambda_{cd}^{kl}\tau_{ij}^{cd}, \quad (29b)$$

$$\gamma_{bj}^{ia} = \lambda_{cb}^{ki}\tau_{kj}^{ca}, \gamma_{ab}^{ij} = \lambda_{ab}^{ij}, \quad (29c)$$

$$\gamma_{ij}^{ab} = \tau_{ij}^{ab}. \quad (29d)$$

In summary, the TD-OCEPA0 method is defined by the EOMs of \hat{T}_2 amplitudes [Eq. (18)] and orbitals [Eq. (25)], with the hole-particle mixing determined by solving Eq. (22) and RDMs given by Eqs. (29).

D. Relation to other ansatz

As the name suggests, the TD-OCEPA0 method is a time-dependent extension of the stationary OCEPA0 method. In the stationary case, it is known that CEPA0^{75,83}, D-MBPT(∞)^{84,85}, third-order expectation value coupled-cluster [XCC(3)]⁸⁶, and the linearized CCD (LCCD)⁸⁷ energy functionals are all equivalent. The similar equivalence in the time-dependent case can be demonstrated by considering the Lagrangian of Eq. (7). In particular, the XCC Lagrangian can be written as

$$\begin{aligned} L &= \frac{1}{\langle \Phi | e^{\hat{T}^\dagger} e^{\hat{T}} | \Phi \rangle} \langle \Phi | e^{\hat{T}^\dagger} (\hat{H} - i\frac{\partial}{\partial t}) e^{\hat{T}} | \Phi \rangle \\ &= \langle \Phi | \left[e^{\hat{T}^\dagger} (\hat{H} - i\frac{\partial}{\partial t}) e^{\hat{T}} \right]_{sc} | \Phi \rangle \\ &\sim \langle \Phi | [(1 + \hat{T}^\dagger)(\hat{H} - i\frac{\partial}{\partial t})(1 + \hat{T})]_{sc} | \Phi \rangle, \\ &= L_0 + \langle \Phi | [(1 + \hat{T}^\dagger)\{\hat{H} - i\hat{X}\}(1 + \hat{T})]_{sc} | \Phi \rangle - i\tau_{ij}^{ab*} \dot{\tau}_{ij}^{ab}, \end{aligned} \quad (30)$$

where $[\dots]_{sc}$ restricts to *strongly connected* terms, and the third line introduces the XCC(3) approximation. This Lagrangian, which leads to the same working equations as derived in Sec. IIC (with $\hat{\Lambda}_2 = \hat{T}_2^\dagger$), emphasizes the Hermitian nature of the TD-OCEPA0, of which a certain advantage over the standard non-Hermitian treatment is discussed in Ref. 88 in the stationary case.

The EOMs of the TD-OCEPA0 method is simpler than those of the closely-related TD-OCCD method (See Appendix A for algebraic details of the TD-OCCD method.) in that all terms quadratic to τ_{ij}^{ab} are absent in the \hat{T}_2 equation [comparing Eq. (18) and (A1)] and in the 2RDM expression [comparing Eq. (29d) and (A3d)]. It should also be noted that one need not solve for $\hat{\Lambda}_2$ for TD-OCEPA0 since $\hat{\Lambda}_2 = \hat{T}_2^\dagger$, in

TABLE I. The ground state total energies of Be and Ne atoms.

Basis	Method	This work ^a	PSI4 ⁸⁰
Be 6-31G ^{*81}	HF	-14.5667 6405	-14.5667 6403
	CEPA0	-14.6192 0336	-14.6192 0335
	OCEPA0	-14.6196 5019	-14.6196 5018
	OCCD	-14.6138 6552	
	OCCDT	-14.6139 4064	
	FCI	-14.6139 4255	-14.6135 4253
Ne cc-pVDZ ⁸¹	HF	-128.4887 7555	-128.4887 7555
	CEPA0	-128.6802 1409	-128.6802 1409
	OCEPA0	-128.6802 9009	-128.6802 9009
	OCCD	-128.6795 9316	
	OCCDT	-128.6807 2135	
	FCI	-128.6808 8113	-128.6808 8113

^a The overlap, one-electron, and two-electron repulsion integrals over Gaussian basis functions are generated using Gaussian09 program (Ref. 82), and used to propagate EOMs in imaginary time in the orthonormalized Gaussian basis, with a convergence threshold of 10^{-15} Hartree of energy difference in subsequent time steps.

contrast to the fact that Eq. (A2) should be solved for TD-OCCD. These simplifications make TD-OCEPA0 computationally much more efficient than TD-OCCD, as numerically demonstrated in Sec. III.

III. NUMERICAL RESULTS AND DISCUSSIONS

A. Ground-state energy

We have implemented the TD-OCEPA0 method for atom-centered Gaussian basis functions and spherical finite-element discrete variable representation (FEDVR) basis for atoms, both with spin-restricted and spin-unrestricted treatments, by modifying the TD-OCCD code described in Ref. 59. Exploiting the feasibility of the imaginary time relaxation to obtain the ground state⁵⁹, we first computed the ground-state energy of Be and Ne atoms with standard Gaussian basis sets, and compare the results with those obtained by PSI4 program package⁸⁰, in which the time-independent OCEPA0 method is implemented. To facilitate the comparison, the number of active spatial orbitals $n_{\text{act}}/2$ are set to be the same as the number of basis functions n_{bas} , since this is the only capability of the PSI4 program. In this case, there are no virtual orbitals (See Sec. II B for the definition.), and therefore, the first term of Eq. (25) vanishes. We also take an option of imaginary-propagating amplitudes only, with all orbitals frozen at the canonical HF solution, to obtain the fixed-orbital CEPA0 energy.

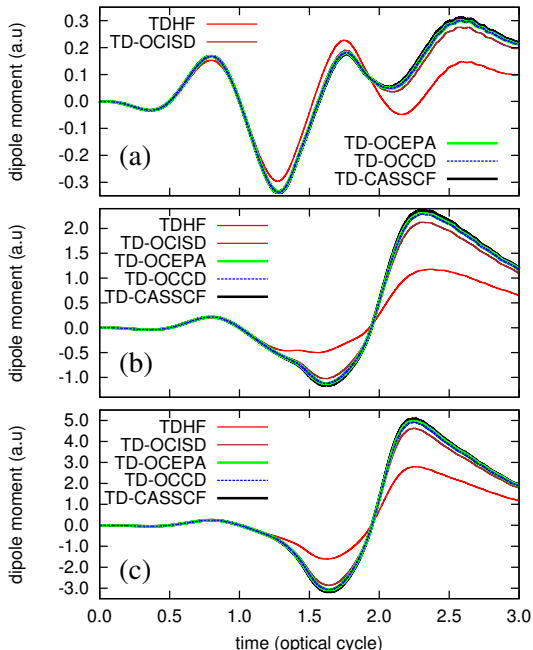


FIG. 1. Time evolution of the dipole moment of Ne irradiated by a laser pulse of a wavelength of 800 nm and intensities of 5×10^{14} W/cm² (a), 8×10^{14} W/cm² (b), and 1×10^{15} W/cm² (c), calculated with TDHF, TD-OCISD, TD-OCEPA, TD-OCCD, and TD-CASSCF methods.

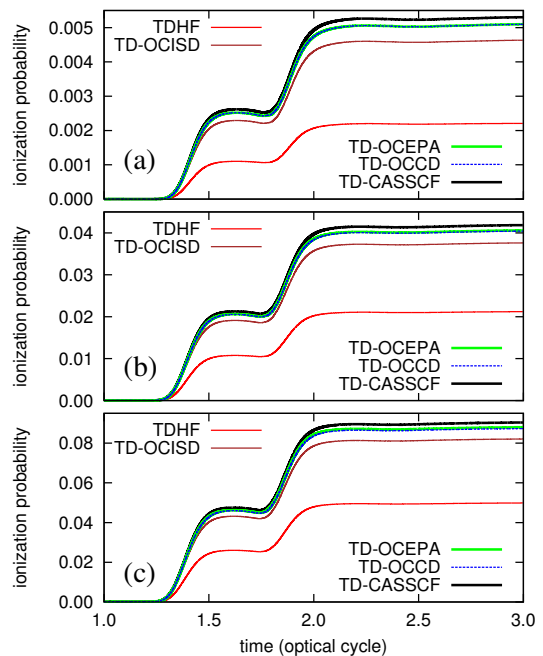


FIG. 2. Time evolution of the single ionization probability of Ne irradiated by a laser pulse of a wavelength of 800 nm and intensities of 5×10^{14} W/cm² (a), 8×10^{14} W/cm² (b), and 1×10^{15} W/cm² (c), calculated with TDHF, TD-OCISD, TD-OCEPA, TD-OCCD, and TD-CASSCF methods.

The calculated total energies listed in Table I demonstrate a virtually perfect agreement of the results of this work and PSI4 program, both for CEPA0 and OCEPA0 methods and for Be and Ne atoms (with a small discrepancy due to a digit truncation of Gaussian one- and two-electron integrals), which confirms the correctness of our implementation.

It is also observed that, for both Be and Ne, the OCEPA0 energies are noticeably lower than the OCCD ones, and for the Be case, the OCEPA0 energy is slightly lower than the FCI energy. Such an overestimation of the correlation energy is usually considered not critical, and more than compensated by the size extensivity in the stationary case.

B. Application to electron dynamics in Ne and Ar

Next, we apply the TD-OCEPA0 method to the laser-driven electron dynamics in Ne and Ar atoms. Within the dipole approximation in the velocity gauge, the one-electron Hamiltonian is given by

$$h(\mathbf{r}, \mathbf{p}) = \frac{1}{2}|\mathbf{p}|^2 - \frac{Z}{|\mathbf{r}|} + A(t)p_z, \quad (31)$$

where Z is the atomic number, $A(t) = -\int^t E(t')dt'$ is the vector potential, with $E(t)$ being the laser electric field linearly polarized along z axis. It should be noted that TD-OCC method (including TD-OCEPA0) is gauge invariant; length-gauge and velocity-gauge simulations, upon numerical convergence, give the same result for observables. The velocity

gauge employed here is advantageous in simulating high-field phenomena^{37,89}.

The laser electric field is given by

$$E(t) = E_0 \sin(\omega_0 t) \sin^2\left(\pi \frac{t}{3T}\right), \quad (32)$$

for $0 \leq t \leq 3T$, and $E(t) = 0$ otherwise, with the central wavelength $\lambda = 2\pi/\omega_0 = 800$ nm, the period $T = 2\pi/\omega_0 \sim 2.67$ fs, and the peak intensity $I_0 = E_0^2$. We consider three different intensities 5×10^{14} W/cm², 8×10^{14} W/cm², and 1×10^{15} W/cm² for Ne, and 2×10^{14} W/cm², 4×10^{14} W/cm², and 6×10^{14} W/cm² for Ar.

The orbital functions are represented by the spherical FEDVR basis^{37,89}, with the maximum angular momentum $l_{\max} = 47$ for Ne and $l_{\max} = 63$ for Ar, and the FEDVR basis supporting the radial coordinate $0 < r < 240$ using 63 finite elements each containing 21 (for Ne) and 23 (for Ar) DVR functions. The absorbing boundary is implemented by a $\cos^{1/4}$ mask function switched on at $r = 180$ to avoid reflection from the box boundary. The ground state of each method is obtained by the imaginary time relaxation, and then the real-time dynamics are simulated starting from the ground state. The Fourth-order exponential Runge-Kutta method⁹⁰ is used to propagate the EOMs with 10000 time steps for each optical cycle.

We compare the performance of the following methods: (i) TDHF, (ii) TD-MCSCF with a TDHF determinant and singly and doubly excited configurations included (TD-OCISD), (iii) TD-OCCD, (iv) TD-OCCDT, and (iv) TD-CASSCF as the fully correlated reference for a given number of active orbitals. In all the methods, the $1s$ orbital of Ne, and $1s2s2p$ orbitals of Ar are kept frozen at the canonical Hartree-Fock orbitals, and for the correlated approaches (ii)-(iv) the eight

valence electrons are correlated among 13 active orbitals. The method (ii) was first introduced in Ref. 40, and referred to as the time-dependent restricted-active-space self-consistent-field method. It can also be considered a specialization of more general time-dependent occupation-restricted multiple-active-space method³⁷. Here we denote the method as TD-OCISD (time-dependent optimized CI with singles and doubles) for simplicity.

The simulation results are given in Figs. 1-3 for Ne and Figs. 4-6 for Ar. For each atom, we report the time evolution of the dipole moment [Figs. 1 and 4], the ionization probability [Figs. 2 and 5], and the HHG spectra [Figs. 3 and 6]. The dipole moment is evaluated as a trace $\langle \psi_p | \hat{z} | \psi_q \rangle \rho_p^q$ using the 1RDM, and the ionization probability is defined as the probability of finding an electron outside a sphere of radius 20 a.u., computed by an expression using 1RDM and 2RDM⁹¹. The HHG spectrum is obtained as the modulus squared $I(\omega) = |a(\omega)|^2$ of the Fourier transform of the expectation value of the dipole acceleration, which, in turn, is obtained with a modified Ehrenfest expression³⁷. The TD-OCCDT results of the dipole moment and the ionization probability are not shown, since they meet a virtually perfect agreement with TD-CASSCF ones. The HHG spectrum is shown only for TDHF, TD-OCEPA0, TD-OCCD, and TD-CASSCF methods [Figs. 3(a)-(c) and 6(a)-(c)] to keep a visibility, and an absolute relative deviation

$$\delta(\omega) = \left| \frac{a(\omega) - a_{\text{TD-CASSCF}}(\omega)}{a_{\text{TD-CASSCF}}(\omega)} \right| \quad (33)$$

of the spectral amplitude $a(\omega)$ from the TD-CASSCF value is reported for each method [Figs. 3(d)-(f) and 6(d)-(f)]. Note that both $I(\omega)$ and $\delta(\omega)$ are plotted in the logarithmic scale, and $\delta(\omega) = 1$ corresponds to a 100% deviation from the TD-CASSCF amplitude.

The dipole moment (Fig. 1) and the ionization probability (Fig. 2) of Ne atom show a general trend that the deviation of results for each method from TD-CASSCF ones decreases as TDHF \gg TD-OCISD $>$ TD-OCEPA0 \approx TD-OCCD $>$ TD-OCCDT. The HHG spectra [Fig. 3 (a)-(c)] are well reproduced by all the methods, except a systematic underestimation of the intensity by TDHF, with the magnitude of the error amounting to 100% of the TD-CASSCF spectral amplitude as shown in Fig. 3 (d)-(f). The magnitude of the error depends weakly on the harmonic order at the plateau region, which decreases again as TDHF \gg TD-OCISD $>$ TD-OCEPA0 \approx TD-OCCD $>$ TD-OCCDT. The Ar atom is characterized by its large ionization potential of 21.6 eV, resulting in relatively low ionization probabilities (Fig. 2) for the present laser pulses. In that case, TD-OCEPA0 and TD-OCCD give a notably similar, and accurate description of dynamics, implying that the truncation after the doubles amplitudes and the linearization of the Lagrangian [Eq. 16] are both justified.

The Ar atom, having a lower ionization potential of 15.6 eV, exhibits a richer dynamics than Ne, e.g. a larger-amplitude

oscillation of the dipole moment (Fig. 4), ionization probabilities as high as 70% (Fig. 5), and HHG spectra characterized by a dip around 34th harmonic related to the Cooper minimum of the photoionization spectrum⁹² at the same energy (Fig. 6). The trend of the accuracy of each method is similar to the case for Ne, except that TD-OCEPA0 and TD-OCCD give noticeably different descriptions of dynamics. In general, TD-OCEPA0 tends to capture a larger part of the correlation effect (the difference between TDHF and TD-CASSCF) than TD-OCCD does. This results in, on one hand, a better agreement of the TD-OCEPA0 results (than TD-OCCD) with TD-CASSCF ones for lower intensity cases [Fig. 4 (a),(b), Fig. 5 (a),(b), and Fig. 6 (d),(e)], and, on the other, leads to an overestimation of the correlation effect for the highest intensity [Fig. 4 (c), Fig. 5 (c), Fig. 6 (f)], somewhat analogous to the overestimation of the ground-state correlation energy as discussed in Sec. III A.

The nonlinear exponential parametrization in TD-OCCD seems to play a role in correcting the overestimation, and the inclusion of the triple excitations (TD-OCCDT) is essential

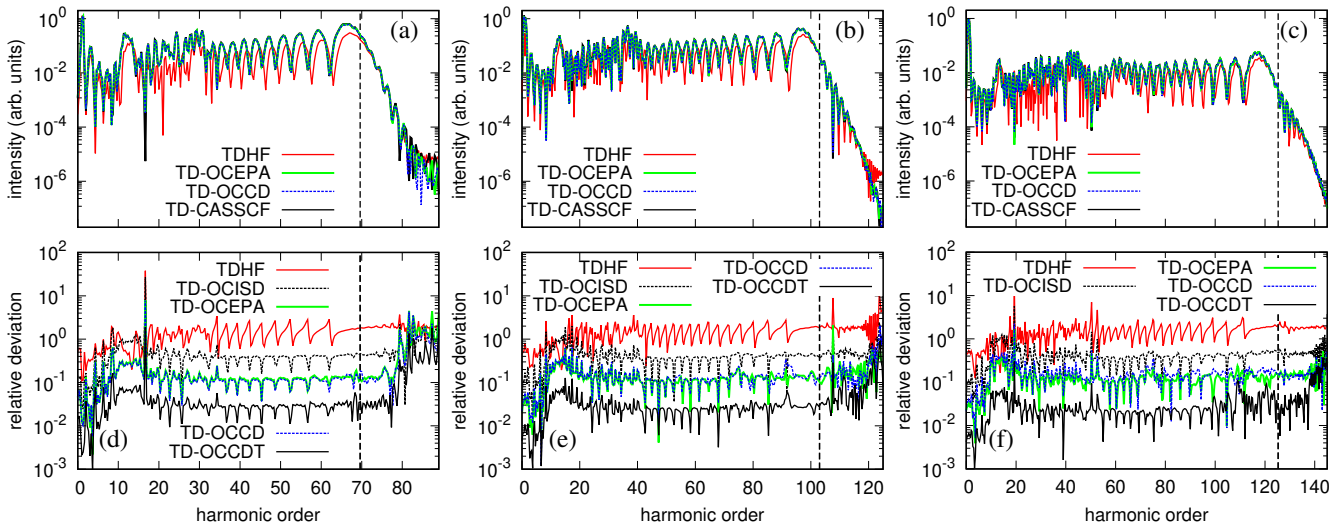


FIG. 3. The HHG spectra from Ne irradiated by a laser pulse of a wavelength of 800 nm obtained with various methods (top), and the relative deviation of the spectral amplitude from the TD-CASSCF spectrum (bottom) defined as Eq. (33), for laser intensities of 5×10^{14} W/cm² (a,d), 8×10^{14} W/cm² (b,e), and 1×10^{15} W/cm² (c,f).

to retain the decisive accuracy across the employed range of the laser intensity. Despite the aforementioned overestimation of the correlation effect for higher intensities, we judge that the present results of TD-OCEPA0 are quite encouraging; it clearly outperforms TD-OCISD for all properties of both atoms, and at least performs equally as TD-OCCD for a

moderate laser intensity.

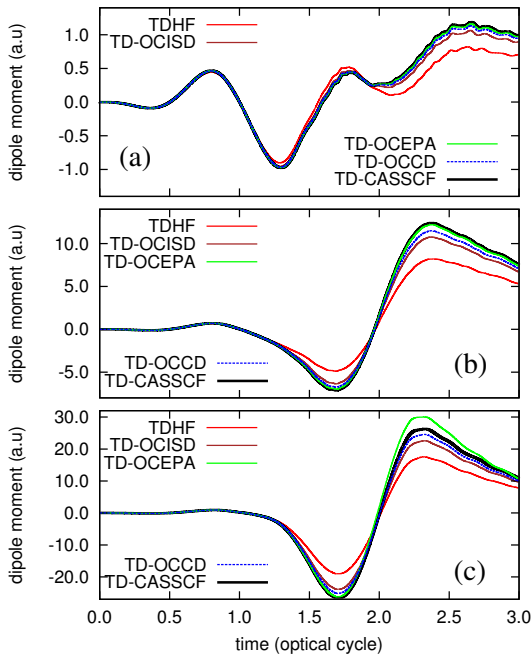


FIG. 4. Time evolution of the dipole moment of Ar irradiated by a laser pulse of a wavelength of 800 nm and intensities of 2×10^{14} W/cm² (a), 4×10^{14} W/cm² (b), and 6×10^{14} W/cm² (c), calculated with TDHF, TD-OCISD, TD-OCEPA, TD-OCCD, and TD-CASSCF methods.

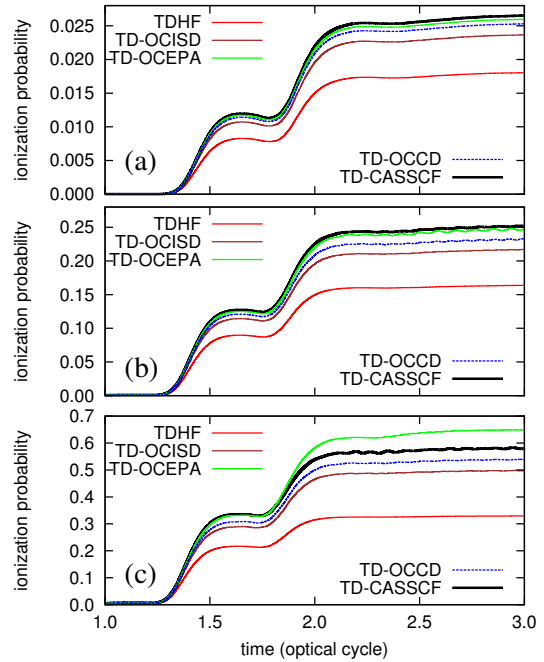


FIG. 5. Time evolution of the single ionization probability of Ar irradiated by a laser pulse of a wavelength of 800 nm and intensities of 2×10^{14} W/cm² (a), 4×10^{14} W/cm² (b), and 6×10^{14} W/cm² (c), calculated with TDHF, TD-OCISD, TD-OCEPA, TD-OCCD, and TD-CASSCF methods.

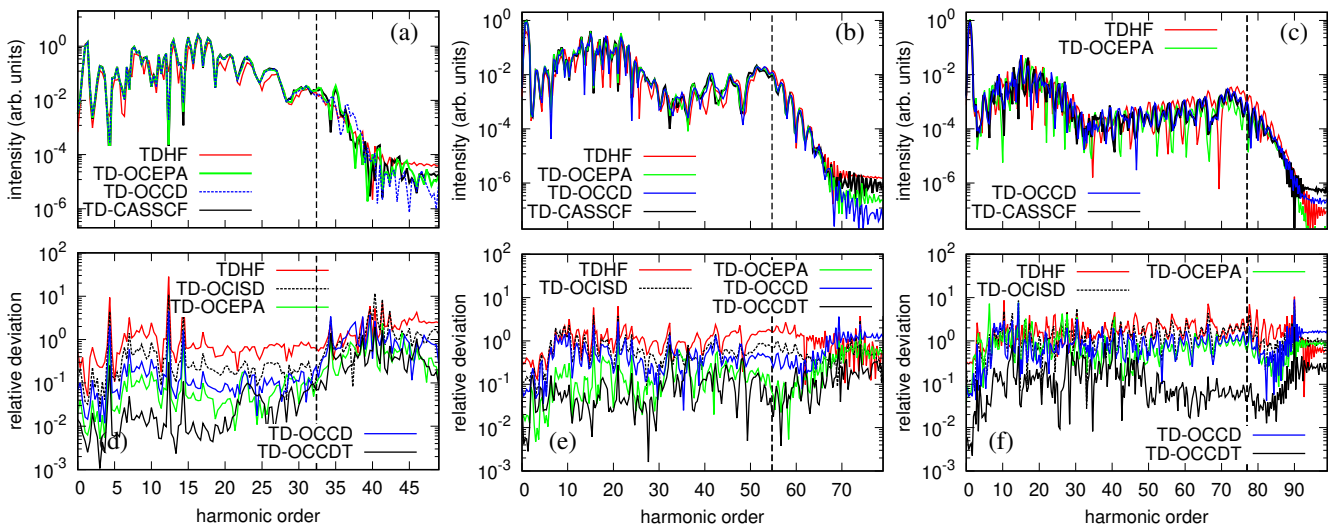


FIG. 6. The HHG spectra from Ar irradiated by a laser pulse of a wavelength of 800 nm obtained with various methods (top), and the relative deviation of the spectral amplitude from the TD-CASSCF spectrum (bottom) defined as Eq. (33), for laser intensities of 2×10^{14} W/cm² (a,d), 4×10^{14} W/cm² (b,e), and 6×10^{14} W/cm² (c,f)

TABLE II. Comparison of the CPU time (in second) spent for the evaluation of the T_2 equation, Λ_2 equation, and 2RDM for TD-OCCD and TD-OCEPA0 methods with various active spaces. See text for more details.

active space ^a	TD-OCCD			TD-OCEPA0		
	T_2	Λ_2	2RDM	T_2	Λ_2	2RDM
(8e-9o)	8.1	11.4	20.7	3.3	-	3.1
(8e-13o)	40.8	55.5	109.4	18.2	-	19.8
(8e-20o)	254.9	332.1	703.9	131.4	-	187.9
(14e-16o)	248.2	307.2	555.5	111.1	-	83.2
(16e-17o)	314.4	437.0	852.1	131.5	-	124.4
(18e-18o)	452.6	619.6	1024.8	187.9	-	143.3

^a CPU time spent for the simulation of Ar atom with n_{act} active orbitals and N_{act} active electrons ($n_{\text{act}}e-N_{\text{act}}o$), recorded and accumulated over 1000 time steps of a real-time simulation ($I_0 = 2 \times 10^{14}$ W/cm² and $\lambda = 800$ nm.), using an Intel(R) Xeon(R) CPU with 12 processors having a clock speed of 3.33GHz.

Finally, we compare the computational cost of TD-OCEPA0 and TD-OCCD methods. Table II reports the central processor unit (CPU) time for the computational bottlenecks differing in these two methods, with varying numbers of active electrons and active orbitals. The largest active space with 18 electrons and 18 orbitals (18e-18o) is challenging for the fully correlated TD-CASSCF.

First, depending on the active space configurations, the evaluation of the \hat{T}_2 equation of the TD-OCEPA0 [Eq. (18)] is 1.9~2.5 times faster than that of TD-OCCD [Eq. (A1)]. A bigger computational gain comes from the fact that one need not solve for the Λ_2 equation, which, for TD-OCCD [Eq. (A2)] takes longer than that for the \hat{T}_2 equation because

of more mathematical operations involved. A further significant cost reduction is obtained by TD-OCEPA0 for the 2RDM evaluation [Eqs. (29d)], which is 5.5~7.2 times faster than the TD-OCCD case [Eqs. (A3d)]. As a whole, the TD-OCEPA0 simulation with, e.g. the (18e-18o) active space achieves 6.3 times speed up relative to the TD-OCCD simulation with the same active orbital space.

IV. SUMMARY

We have presented the implementation of TD-OCEPA0 method as a cost-effective approximation within the TD-OCC framework, for the first principles study of intense laser-driven multielectron dynamics. The TD-OCEPA0 method retains the important size-extensivity and gauge-invariance of TD-OCC, and computationally much more efficient than the full TD-OCCD method. As a first numerical test, we applied the present implementation to Ne and Ar atoms irradiated by an intense near infrared laser pulses with three different intensities to compare the time-dependent dipole moment, the ionization probability, and HHG spectra with those obtained with other methods including the fully correlated TD-CASSCF methods with the same number of active orbitals. It is observed that, for the highest laser intensity, with sizable ionization, the TD-OCEPA0 tends to overestimate the correlation effect defined as the difference between TDHF and TD-CASSCF descriptions. For moderate intensities, however, the TD-OCEPA0 method performs at least equally well as TD-OCCD with a substantially lower computational cost. It is anticipated that the present TD-OCEPA0 method serves as an important theoretical tool to investigate ultrafast and/or high-field processes in chemically relevant large molecular systems.

ACKNOWLEDGMENTS

This research was supported in part by a Grant-in-Aid for Scientific Research (Grants No. 16H03881, No. 17K05070, No. 18H03891, and No. 19H00869) from the Ministry of Education, Culture, Sports, Science and Technology (MEXT) of Japan. This research was also partially supported by JST COI (Grant No. JPMJCE1313), JST CREST (Grant No. JPMJCR15N1), and by MEXT Quantum Leap Flagship Program (MEXT Q-LEAP) Grant Number JPMXS0118067246.

Appendix A: Algebraic details of TD-OCCD

The TD-OCCD method implemented in Ref. 59 employs the same truncation ($\hat{T} = \hat{T}_2$ and $\hat{\Lambda} = \hat{\Lambda}_2$) as for TD-OCEPA0, but retains the full exponential operator $e^{\hat{T}_2}$. As a result, the amplitude EOMs are given by

$$\begin{aligned} i\dot{\tau}_{ij}^{ab} &= v_{ij}^{ab} - p(ij)\bar{f}_j^k\tau_{ik}^{ab} + p(ab)\bar{f}_c^a\tau_{ij}^{cb} \\ &+ \frac{1}{2}v_{cd}^{ab}\tau_{ij}^{cd} + \frac{1}{2}v_{ij}^{kl}\tau_{kl}^{ab} + p(ij)p(ab)v_{ic}^{ak}\tau_{kj}^{cb} \\ &- \frac{1}{2}p(ij)\tau_{ik}^{ab}\tau_{jl}^{cd}v_{cd}^{kl} + \frac{1}{2}p(ab)\tau_{ij}^{bc}\tau_{kl}^{ad}v_{cd}^{kl} \\ &+ \frac{1}{4}\tau_{kl}^{ab}\tau_{ij}^{cd}v_{cd}^{kl} + \frac{1}{2}p(ij)p(ab)\tau_{il}^{bc}\tau_{jk}^{ad}v_{cd}^{kl}, \end{aligned} \quad (\text{A1})$$

$$\begin{aligned} -i\dot{\lambda}_{ab}^{ij} &= v_{ab}^{ij} - p(ij)\bar{f}_i^k\lambda_{ab}^{kj} + p(ab)\bar{f}_a^c\lambda_{cb}^{ij} \\ &+ \frac{1}{2}v_{ab}^{cd}\lambda_{cd}^{ij} + \frac{1}{2}v_{kl}^{ij}\lambda_{ab}^{kl} + p(ij)p(ab)v_{kb}^{cj}\lambda_{ac}^{ik} \\ &- \frac{1}{2}p(ij)\lambda_{cd}^{ik}\tau_{kl}^{cd}v_{ab}^{jl} + \frac{1}{2}p(ab)\lambda_{bc}^{kl}\tau_{kl}^{cd}v_{ad}^{ij} \\ &+ \frac{1}{4}\lambda_{ab}^{kl}\tau_{kl}^{cd}v_{cd}^{ij} + \frac{1}{2}p(ij)p(ab)\lambda_{ac}^{jk}\tau_{kl}^{cd}v_{bd}^{il} \\ &- \frac{1}{2}p(ij)\lambda_{ab}^{ik}\tau_{kl}^{cd}v_{cd}^{jl} + \frac{1}{2}p(ab)\lambda_{bc}^{ij}\tau_{kl}^{cd}v_{ad}^{kl} \\ &+ \frac{1}{4}\lambda_{cd}^{ij}\tau_{kl}^{cd}v_{ab}^{kl}. \end{aligned} \quad (\text{A2})$$

The EOMs for orbitals are formally the same as that for TD-OCEPA0, Eqs. (25)-(27), but with RDMs ρ replaced with Hermitalized ones, $D_q^p = (\rho_q^p + \rho_p^{q*})/2$ and $P_{qs}^{pr} = (\rho_{qs}^{pr} + \rho_{pr}^{qs*})/2$. Finally the algebraic expression for non-zero correlation RDM elements is

$$\gamma_i^j = -\frac{1}{2}\lambda_{cd}^{kj}\tau_{ki}^{cd}, \gamma_a^b = \frac{1}{2}\lambda_{ca}^{kl}\tau_{kl}^{cb}, \quad (\text{A3a})$$

$$\gamma_{ab}^{cd} = \frac{1}{2}\lambda_{ab}^{kl}\tau_{kl}^{cd}, \gamma_{ij}^{kl} = \frac{1}{2}\lambda_{cd}^{kl}\tau_{ij}^{cd}, \quad (\text{A3b})$$

$$\gamma_{bj}^{ia} = \lambda_{cb}^{ki}\tau_{kj}^{ca}, \gamma_{ab}^{ij} = \lambda_{ab}^{ij}, \quad (\text{A3c})$$

$$\begin{aligned} \gamma_{ij}^{ab} &= \tau_{ij}^{ab} + \frac{1}{2}p(ij)p(ab)\lambda_{cd}^{kl}\tau_{ki}^{ca}\tau_{jl}^{bd} \\ &- \frac{1}{2}p(ij)\lambda_{cd}^{kl}\tau_{ki}^{cd}\tau_{lj}^{ab} - \frac{1}{2}p(ab)\lambda_{cd}^{kl}\tau_{kl}^{ca}\tau_{ij}^{db} \\ &+ \frac{1}{4}\lambda_{cd}^{kl}\tau_{ij}^{cd}\tau_{kl}^{ab}. \end{aligned} \quad (\text{A3d})$$

- ¹M. Schultze *et al.*, *Science* **328**, 1658 (2010).
- ²K. Klünder *et al.*, *Physical Review Letters* **106**, 143002 (2011).
- ³L. Belshaw *et al.*, *The journal of physical chemistry letters* **3**, 3751 (2012).
- ⁴F. Calegari *et al.*, *Science* **346**, 336 (2014).
- ⁵J. Itatani *et al.*, *Nature* **432**, 867 (2004).
- ⁶O. Smirnova *et al.*, *Nature* **460**, 972 (2009).
- ⁷S. Haessler *et al.*, *Nature Physics* **6**, 200 (2010).
- ⁸M. Protopapas, C. H. Keitel, and P. L. Knight, *Reports on Progress in Physics* **60**, 389 (1997).
- ⁹F. Krausz and M. Ivanov, *Rev. Mod. Phys.* **81**, 163 (2009).
- ¹⁰P. Agostini and L. F. DiMauro, *Reports on progress in physics* **67**, 813 (2004).
- ¹¹L. Gallmann, C. Cirelli, and U. Keller, *Annual review of physical chemistry* **63**, 447 (2012).
- ¹²Z. Chang, *Fundamentals of attosecond optics* (CRC press, 2016).
- ¹³K. Zhao *et al.*, *Optics letters* **37**, 3891 (2012).
- ¹⁴E. J. Takahashi, P. Lan, O. D. Mücke, Y. Nabekawa, and K. Midorikawa, *Nature communications* **4**, 2691 (2013).
- ¹⁵T. Popmintchev *et al.*, *science* **336**, 1287 (2012).
- ¹⁶P. M. Kraus *et al.*, *Science* **350**, 790 (2015).
- ¹⁷K. L. Ishikawa, *Advances in Solid State Lasers Development and Applications* (InTech, 2010), chap. High-Harmonic Generation.
- ¹⁸K. L. Ishikawa and T. Sato, *IEEE Journal of Selected Topics in Quantum Electronics* **21**, 1 (2015).
- ¹⁹J. S. Parker, E. S. Smyth, and K. T. Taylor, *Journal of Physics B: Atomic, Molecular and Optical Physics* **31**, L571 (1998).
- ²⁰J. S. Parker *et al.*, *Journal of Physics B: Atomic, Molecular and Optical Physics* **33**, L239 (2000).
- ²¹M. Pindzola and F. Robicheaux, *Physical Review A* **57**, 318 (1998).
- ²²S. Laulan and H. Bachau, *Physical Review A* **68**, 013409 (2003).
- ²³K. L. Ishikawa and K. Midorikawa, *Physical Review A* **72**, 013407 (2005).
- ²⁴J. Feist *et al.*, *Physical review letters* **103**, 063002 (2009).
- ²⁵K. L. Ishikawa and K. Ueda, *Physical review letters* **108**, 033003 (2012).
- ²⁶S. Sukiasyan, K. L. Ishikawa, and M. Ivanov, *Physical Review A* **86**, 033423 (2012).
- ²⁷W. Vanroose, D. A. Horner, F. Martin, T. N. Rescigno, and C. W. McCurdy, *Physical Review A* **74**, 052702 (2006).
- ²⁸D. A. Horner *et al.*, *Physical review letters* **101**, 183002 (2008).
- ²⁹J. Krause, *Phys. Rev. Lett.* **68**, 3535 (1992).
- ³⁰K. C. Kulander, *Physical Review A* **36**, 2726 (1987).
- ³¹J. Caillat *et al.*, *Physical review A* **71**, 012712 (2005).
- ³²T. Kato and H. Kono, *Chemical physics letters* **392**, 533 (2004).
- ³³M. Nest, T. Klamroth, and P. Saalfrank, *The Journal of chemical physics* **122**, 124102 (2005).
- ³⁴D. J. Haxton, K. V. Lawler, and C. W. McCurdy, *Physical Review A* **83**, 063416 (2011).
- ³⁵D. Hochstuhl and M. Bonitz, *The Journal of chemical physics* **134**, 084106 (2011).
- ³⁶T. Sato and K. L. Ishikawa, *Physical Review A* **88**, 023402 (2013).
- ³⁷T. Sato *et al.*, *Physical Review A* **94**, 023405 (2016).
- ³⁸I. Tikhomirov, T. Sato, and K. L. Ishikawa, *Physical review letters* **118**, 203202 (2017).
- ³⁹H. Miyagi and L. B. Madsen, *Physical Review A* **87**, 062511 (2013).
- ⁴⁰H. Miyagi and L. B. Madsen, *Physical Review A* **89**, 063416 (2014).
- ⁴¹D. J. Haxton and C. W. McCurdy, *Physical Review A* **91**, 012509 (2015).
- ⁴²T. Sato and K. L. Ishikawa, *Physical Review A* **91**, 023417 (2015).
- ⁴³I. Shavitt and R. J. Bartlett, *Many-body methods in chemistry and physics: MBPT and coupled-cluster theory* (Cambridge university press, 2009).
- ⁴⁴H. G. Kümmer, *International Journal of Modern Physics B* **17**, 5311 (2003).
- ⁴⁵T. D. Crawford and H. F. Schaefer, *Reviews in Computational Chemistry*, Volume 14, 33 (2007).
- ⁴⁶K. Schonhammer, *Phys. Rev. B* **18**, 6606 (1978).
- ⁴⁷P. Hoodbhoy and J. W. Negele, *Physical Review C* **18**, 2380 (1978).
- ⁴⁸P. Hoodbhoy and J. W. Negele, *Physical Review C* **19**, 1971 (1979).
- ⁴⁹E. Dalgaard and H. J. Monkhorst, *Physical Review A* **28**, 1217 (1983).
- ⁵⁰H. Koch and P. Joergensen, *The Journal of Chemical Physics* **93**, 3333 (1990).
- ⁵¹M. Takahashi and J. Paldus, *The Journal of chemical physics* **85**, 1486 (1986).
- ⁵²M. D. Prasad, *The Journal of chemical physics* **88**, 7005 (1988).

- ⁵³K. Sebastian, *Physical Review B* **31**, 6976 (1985).
- ⁵⁴D. A. Pigg, G. Hagen, H. Nam, and T. Papenbrock, *Physical Review C* **86**, 014308 (2012).
- ⁵⁵D. R. Nascimento and A. E. DePrince III, *Journal of chemical theory and computation* **12**, 5834 (2016).
- ⁵⁶C. Huber and T. Klamroth, *The Journal of chemical physics* **134**, 054113 (2011).
- ⁵⁷S. Kvaal, *The Journal of chemical physics* **136**, 194109 (2012).
- ⁵⁸J. Arponen, *Annals of Physics* **151**, 311 (1983).
- ⁵⁹T. Sato, H. Pathak, Y. Orimo, and K. L. Ishikawa, *The Journal of chemical physics* **148**, 051101 (2018).
- ⁶⁰G. E. Scuseria and H. F. Schaefer III, *Chemical physics letters* **142**, 354 (1987).
- ⁶¹C. D. Sherrill, A. I. Krylov, E. F. Byrd, and M. Head-Gordon, *The Journal of chemical physics* **109**, 4171 (1998).
- ⁶²A. I. Krylov, C. D. Sherrill, E. F. Byrd, and M. Head-Gordon, *The Journal of chemical physics* **109**, 10669 (1998).
- ⁶³G. D. Lindh, T. J. Mach, and T. D. Crawford, *Chemical Physics* **401**, 125 (2012).
- ⁶⁴R. H. Myhre, *The Journal of chemical physics* **148**, 094110 (2018).
- ⁶⁵T. B. Pedersen and S. Kvaal, *The Journal of chemical physics* **150**, 144106 (2019).
- ⁶⁶T. B. Pedersen, H. Koch, and C. Hättig, *The Journal of chemical physics* **110**, 8318 (1999).
- ⁶⁷T. B. Pedersen, B. Fernandez, and H. Koch, *The Journal of chemical physics* **114**, 6983 (2001).
- ⁶⁸W. Meyer, *International Journal of Quantum Chemistry* **5**, 341 (1971).
- ⁶⁹W. Meyer, *Methods of electronic structure theory*, 1977.
- ⁷⁰H.-J. Werner and W. Meyer, *Molecular Physics* **31**, 855 (1976).
- ⁷¹R. Ahlrichs, P. Scharf, and C. Ehrhardt, *The Journal of Chemical Physics* **82**, 890 (1985).
- ⁷²P. Pulay and S. Sæbø, *Chemical physics letters* **117**, 37 (1985).
- ⁷³R. Ahlrichs, F. Driessler, H. Lischka, V. Staemmler, and W. Kutzelnigg, *The Journal of Chemical Physics* **62**, 1235 (1975).
- ⁷⁴S. Koch and W. Kutzelnigg, *Theoretica chimica acta* **59**, 387 (1980).
- ⁷⁵F. Wennmohs and F. Neese, *Chemical Physics* **343**, 217 (2008).
- ⁷⁶F. Neese, F. Wennmohs, and A. Hansen, *The Journal of chemical physics* **130**, 114108 (2009).
- ⁷⁷C. Kollmar and F. Neese, *Molecular Physics* **108**, 2449 (2010).
- ⁷⁸J.-P. Malrieu, H. Zhang, and J. Ma, *Chemical Physics Letters* **493**, 179 (2010).
- ⁷⁹U. Bozkaya and C. D. Sherrill, *The Journal of chemical physics* **139**, 054104 (2013).
- ⁸⁰J. M. Turney *et al.*, *Wiley Interdisciplinary Reviews: Computational Molecular Science* **2**, 556 (2012).
- ⁸¹J. D. Dill and J. A. Pople, *The Journal of Chemical Physics* **62**, 2921 (1975).
- ⁸²M. Frisch *et al.*, *Gaussian 09*, revision d. 01, 2009.
- ⁸³R. Ahlrichs, *Computer Physics Communications* **17**, 31 (1979).
- ⁸⁴R. J. Bartlett and I. Shavitt, *Chemical Physics Letters* **50**, 190 (1977).
- ⁸⁵R. J. Bartlett, I. Shavitt, and G. D. Purvis III, *The Journal of Chemical Physics* **71**, 281 (1979).
- ⁸⁶R. J. Bartlett and J. Noga, *Chemical physics letters* **150**, 29 (1988).
- ⁸⁷R. J. Bartlett, *Annual Review of Physical Chemistry* **32**, 359 (1981).
- ⁸⁸A. G. Taube and R. J. Bartlett, *The Journal of chemical physics* **130**, 144112 (2009).
- ⁸⁹Y. Orimo, T. Sato, A. Scrinzi, and K. L. Ishikawa, *Physical Review A* **97**, 023423 (2018).
- ⁹⁰M. Hochbruck and A. Ostermann, *Acta Numerica* **19**, 209 (2010).
- ⁹¹F. Lackner, I. Březinová, T. Sato, K. L. Ishikawa, and J. Burgdörfer, *Physical Review A* **91**, 023412 (2015).
- ⁹²J. Wörner, Hans, H. Niikura, J. B. Bertrand, P. Corkum, and D. Villeneuve, *Phys. Rev. Lett.* **102**, 103901 (2009).